Molecular Structure and Dynamics in the Low Temperature (Orthorhombic) Phase of NH_3BH_3

Herman Cho,* Wendy J. Shaw, Vencislav Parvanov, Gregory K. Schenter, Abhijeet Karkamkar, Nancy J. Hess, Chris Mundy, Shawn Kathmann, Jesse Sears, Andrew S. Lipton, Paul D. Ellis, and S. Thomas Autrey*

Fundamental and Computational Sciences Directorate, Pacific Northwest National Laboratory, P. O. Box 999, Richland, Washington 99352

Received: December 14, 2007; In Final Form: February 14, 2008

Variable temperature ^{2}H NMR experiments on the orthorhombic phase of selectively deuterated NH_3BH_3 spanning the static to fast exchange limits of the borane and amine motions are reported. New values of the electric field gradient (EFG) tensor parameters have been obtained from the static ^{2}H spectra of $V_{zz} = 1.652$ ($\pm$0.082) $\times$ 10^{21} V/m^2 and $\eta = 0.00 \pm 0.05$ for the borane hydrogens and $V_{zz} = 2.883$ ($\pm$0.144) $\times$ 10^{21} V/m^2 and $\eta = 0.00 \pm 0.05$ for the amine hydrogens. The molecular symmetry inferred from the observation of equal EFG tensors for the three borane hydrogens and likewise for the three amine hydrogens is in sharp contrast with the C_s symmetry derived from diffraction studies. The origin of the apparent discrepancy has been investigated using molecular dynamics methods in combination with electronic structure calculations of NMR parameters, bond lengths, and bond angles. The computation of parameters from a statistical ensemble rather than from a single set of atomic Cartesian coordinates gives values that are in close quantitative agreement with the ^{2}H NMR electric field gradient tensor measurements and are more consistent with the molecular symmetry revealed by the NMR spectra.

1. Introduction

The promising attributes of solid NH_3BH_3 as a hydrogen storage medium[1] and the unusual intermolecular interactions of the boraneamines[2] have raised interest in the molecule's hydrogen bonding and dynamics in the solid state. Rotational motions of the NH_3 and BH_3 groups in particular have been probed by a number of techniques, both in the gas and in the condensed phases.[3−6] The temperature dependence of ^{2}H NMR lineshapes and relaxation times has been previously recognized by Penner et al.[5] as providing an informative picture of molecular dynamics below the tetragonal/orthorhombic phase transition temperature of 225 K. However, the temperature series they presented was incomplete, stopping at a lower limit of 110 K, which did not allow them to take full advantage of the range of time scales accessible to ^{2}H NMR methods, particularly in the slow motion regime ($\tau_c > 10^{-5}$ s). Furthermore, lacking ^{2}H spectra in the static limit, the electric field gradient (EFG) tensors could not be determined directly and were instead inferred from motionally averaged lineshapes acquired in the high temperature, fast exchange limit.

The ^{2}H NMR lineshapes of NH_3BD_3 observed in this prior work indicate that the three deuterons have equal quadrupolar couplings, and moreover, their EFG tensors are axially symmetric ($\eta_Q \approx 0$), with similar conclusions for ND_3BH_3. But while these findings are plausible for an isolated molecule with a threefold axis of symmetry, they are at first glance incompatible with a molecule that interacts asymmetrically with its neighbors through hydrogen bonds[2] in an orthorhombic environment. In the intervening time since the publication of these results, more complete determinations of atomic and lattice coordinates have become available from powder diffraction measurements, making it possible to compute nuclear parameters such as EFG tensors using actual experimental inputs to specify the molecule's structure and local environment. These new data reveal a significant deviation from C_{3v} symmetry and appear to reinforce the expectation that the geometry of the molecule in the orthorhombic phase precludes the symmetry implied by the ^{2}H NMR spectra.

The NMR and diffraction measurements that lead to these contradictions are fundamentally statistical in nature, and to put a theoretical analysis of these data on an equal, consistent footing, statistical averaging of computed structural and NMR parameters must be considered for systems down to the low-temperature, static limit. In addition to more closely representing the measurement process, averaging of computed parameters clarifies the relationship between geometric parameters obtained, for example, by NMR spectroscopy, and lattice coordinates determined by diffraction methods, and represents a way to reconcile the differences in molecular structures inferred from the two approaches.

2. Experimental Methods

Preparation of ND_3BH_3. One gram of NH_3BH_3 was dissolved in 10 mL D_2O, stirred for 10−15 min, and the water was removed by rotary evaporation. This was repeated three times to complete the exchange of the amine protons with deuterium.

Preparation of NH_3BD_3. Equimolar ratios of $NaBH_4$ and $N(CH_3)_3Cl$ were dissolved. The resulting $(CH_3)_3NBH_3$ was dissolved in ether, deuterated with D_2O, and acidified with DCl to give $(CH_3)_3NBD_3$. The deuterated product was then mixed with $NaOCH_3$ in diglyme to yield NH_3BD_3.

* Corresponding authors. E-mail: tom.autrey@pnl.gov (S.T.A.).

10.1021/jp7117696 CCC: $40.75
Published on Web 04/12/2008

NMR Spectroscopy. Polycrystalline samples were packed into 5 mm glass tubes in a glovebox, frozen, pumped, thawed, and degassed under 10^{-4} Torr vacuum, and finally flame-sealed to prevent oxygen contamination. Spin−lattice (T_1) relaxation times were determined by the inversion recovery method with quadrupolar echo detection of the recovered magnetization. Data were fit to a single exponential. Measurements from 120 to 220 K were acquired at 7.06 T (46.267 MHz for ^{2}H) on a Chemagnetics Infinity spectrometer utilizing a Chemagnetics probe. The 90° pulse time was 2.5 μs. The temperature was measured prior to measurements with a thermocouple inserted into the sample coil.

Low temperature (<140 K) ^{2}H spectra were recorded at 9.4 T (61.394 MHz) by the quadrupolar echo method (dephasing delay = 35 μs) on a Varian InfinityPlus spectrometer utilizing a home-built low-temperature probe.[7] Ninety degree pulse widths were calibrated at 150 K and calculated at other temperatures based on the measured quality factor of the probe, assuming the approximate proportionality of B_1 with Q. Typical pulse times determined in this way ranged from 1.9 (11 K) to 2.4 μs (160 K). Recycle delays were set to at least five times the measured T_1. The temperature was measured continuously, 15 mm from the sample. Identical instrument settings were used for all experiments.

Because of the extreme lengthening of T_1 at low temperatures, the ND_3BH_3 spectrum measured at 11 K was collected by warming the sample to 70 K between scans, where the T_1 was 4 s, and allowing the sample to fully polarize at this temperature before returning the sample to 11 K for the next acquisition. The cycling process took 30 to 60 min, compared with the T_1 at 11 K obtained by extrapolation of >160 h.

3. Computational Methods

Static Spectrum Simulations. Simulated time domain ^{2}H NMR interferograms were computed numerically by the time-dependent density matrix formalism,[8] and then Fourier transformed to obtain spectra. The high field internal Hamiltonian $\mathscr{H}_{\text{int}}$ was assumed to consist of a quadrupolar term evaluated to first order[9] and a secular heteronuclear dipolar coupling term.[10] Evolution during radiofrequency (rf) pulse periods was computed with a total static Hamiltonian that included $\mathscr{H}_{\text{int}}$ in addition to the rf interaction term. Pulse times, rf field amplitudes, dephasing delays, spectral width, and other parameters under experimental control were set equal to the values used in actual experiments. Powder spectra were obtained by computing and summing interferograms for 10 300 orientations chosen according to the algorithm of Mombourquette and Weil.[11] The ^{2}H quadrupole moment value of 0.00286×10^{-24} cm^2 recommended by Raghavan[12] was used to convert deuterium quadrupolar coupling constants to electric field gradients and vice versa. The C^{++} programs written for these calculations incorporate objects from the mathematical shell of the GAMMA version 4.1.0 NMR simulation environment.[13]

^{2}H Dynamical Line Shape Simulations. A Mathematica program was created to compute the effects of anisotropic motion on the ^{2}H time domain NMR signal following the method of Anderson,[14,15] modified to account for quadrupolar echo detection and unrefocused T_2 decay.[16] The dephasing delay in the calculation was matched to the values used in experiments.

Single Configuration Parameter Calculations. Electric field gradient tensors of single configurations of molecules were computed from the electron density using the implemented procedure in the Gaussian program[17] with the B3LYP method[18] and basis set.[19] Structures were optimized where noted within the Gaussian program with applied restriction on the B−N bond relaxation. In these calculations, the B−N bond was fixed to the distance determined by neutron diffraction (ND) at 200 K.[2] Alternatively, the geometry of the molecule at 200 K was transformed to C_{3v} symmetry by averaging of the respective bonds and angles of the hydrogen atoms of BH_3 and NH_3. The molecular geometries and intermolecular distances were not optimized in the cluster calculations.

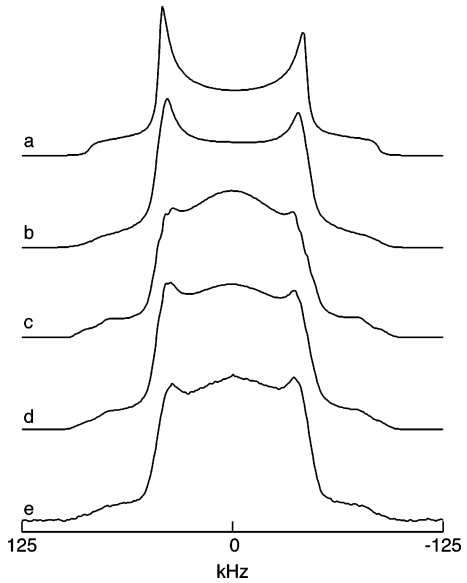

Figure 1. Simulated and experimental ^{2}H NMR quadrupolar echo spectra of NH_3BD_3 in the static limit. (a) Simulation with quadrupolar interaction only; (b) simulation including dipolar coupling to ^{10}B; (c) simulation including dipolar coupling to ^{11}B; (d) sum of b and c weighted according to isotopic abundances of ^{10}B (19.6%) and ^{11}B (80.4%); (e) experimental spectrum measured at 90 K.

Calculations of Statistical Averages. Ensemble averages of EFG parameters, bond lengths, and bond angles were evaluated by performing a series of periodic density functional theory (DFT) electronic structure calculations to generate an ensemble of configurations corresponding to temperatures of 15 and 120 K. The time evolution of a canonical ensemble consisting of a 16-molecule periodic cell was simulated with the CP2K code.[20,21] A PBE functional[22] was used with a TZVP basis set[21] and Goedecker pseudopotentials.[23,24] 150 000 simulation steps of a Nose bath dynamics with a 0.5 fs time step was used to generate an ensemble of configurations for averaging. The periodic simulation cell was chosen to be consistent with preliminary Rietveld analysis of neutron diffraction results [$Pmn2_1$, $Z = 2$; 15 K, (11.09114, 9.23686, 9.98501) Å; 120 K, (11.00684, 9.47054, 10.01873) Å].[25] Electric field gradient tensors were computed within the CP2K code for 30 representative configurations from the ensemble with a BLYP functional and a 6-31ppG3f2d basis set. The mean value and statistical distribution of parameters consistent with the ensemble could both be determined by this approach.

4. Results and Discussion

Deuterium EFG Tensors. Deuterium NMR quadrupolar echo spectra of polycrystalline NH_3BD_3 and ND_3BH_3 appear in Figures 1 and 2, respectively. Variable temperature lineshape and relaxation time measurements indicate that the rates of molecular rotations are very slow (<10^3 s^{-1}) below 100 K (for $-BH_3$) and 60 K (for $-NH_3$), and the experimental spectra in these figures represent static limits.

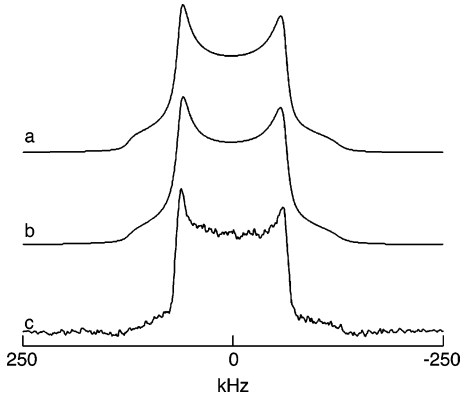

Figure 2. Simulated and experimental ^{2}H NMR quadrupolar echo spectra of ND_3BH_3 in the static limit. (a) Simulation with quadrupolar interaction only; (b) simulation including dipolar coupling to ^{14}N; (c) experimental spectrum measured at 11 K.

Deviations from the classic Pake powder lineshape of an isolated spin-1 nuclide[15] are visible in both figures. The simulated spectra in Figures 1 and 2 show that these distortions can be explained by dipolar couplings to nearby nuclei. The effects are most pronounced for NH_3BD_3 because of the large gyromagnetic ratio of ^{11}B, the short B−H internuclear distance, and the smaller ^{2}H quadrupolar interaction in NH_3BD_3 relative to ND_3BH_3. In the absence of a classic Pake lineshape, spectral simulations that include the dipolar interaction allow a more accurate determination of the hydrogen EFG tensor in the static limit, especially for NH_3BD_3.

The simulated spectra were adjusted for best visual fit to the experimental result by varying V_{zz}, that is, the gradient in the z principal direction of the z component of the electric field at the deuteron position, and the homogeneous linebroadening. The Hamiltonian in the spectral simulations consisted of the deuteron's quadrupolar interaction and the heteronuclear coupling to the directly bonded ^{10}B, ^{11}B, or ^{14}N. Internuclear distances from molecular dynamics calculations (vide infra) were used in computations of heteronuclear dipolar couplings. The slight asymmetry in all of the spectra is due to finite pulse width effects of the quadrupolar echo excitation sequence.

It has been assumed in the simulations of Figures 1 and 2 that the three hydrogens of NH_3BD_3 have identical, axially symmetric EFG tensors, oriented in like fashion with the z principal axes parallel to the B−D bonds, and likewise for the three hydrogens in ND_3BH_3. If the EFG tensors were not equivalent, each deuteron would give rise to a different powder lineshape; in simulations with comparable homogeneous linebroadening, we find that overlapped powder lineshapes become distinguishable if the difference in V_{zz} is 5% or greater. No sign of multiple powder lineshapes is observed in the experimental spectra of either NH_3BD_3 or ND_3BH_3.

The EFG tensor parameters V_{zz} and η extracted from the fits of the experimental spectra are collected in Table 1 (first data column), along with values calculated by a variety of different methods. The second data column contains computed results for an isolated, optimized molecule; because environmental effects were not included, optimization of the structure naturally produces a molecular geometry with C_{3v} symmetry. The third data column also displays computed results but for a structure determined by neutron diffraction. The atomic coordinates from this work indicate a molecular geometry with C_s symmetry instead of C_{3v} in the orthorhombic lattice, and accordingly both the borane and the amine groups are characterized by two H atoms positioned above and below the mirror plane and one inequivalent H atom lying within the mirror plane. The inequivalence of the in- and out-of-plane sites is reflected in calculated values of V_{zz} that differ by −121% and 12% for the amine and borane hydrogens, respectively, contrary to the ^{2}H NMR spectra, which reveal no differences of these magnitudes. A statistical treatment that gives the fourth and fifth data columns in Table 1 is considered in the next section as the explanation for this apparent inconsistency in NMR and ND findings.

The surfaces in Figure 3 illustrate the sensitivity of V_{zz} to the hydrogen coordinates in a symmetrized molecular geometry. For both the borane and the amine hydrogens, V_{zz} is found to be strongly dependent on d_{BH} and d_{NH}, respectively, while being nearly invariant over a wide range of bond angles. Similar trends have been observed in a computational study by Penner et al.[5] From these plots, it can be estimated that modifying d_{BH} of the isolated molecule by 0.026 Å can bring the computed value of V_{zz} into agreement with the NMR measurement, and likewise, adjustment of d_{NH} by 0.028 Å leads to a calculated value of V_{zz} that is equal to the measured result. These results demonstrate the importance of accurate hydrogen coordinates in calculating reliable EFG tensors and suggest that differences in measured and calculated values of V_{zz} can be reconciled by adjustments that are within the uncertainty of the bond distances.

Effects of Statistical Averaging. The analysis of the ^{2}H NMR data relies on the important assumptions that the B−N bond is an axis of three-fold symmetry for the molecular structure, and the z principal axis of the hydrogen EFG tensor is aligned along the B−H (or N−H) bond. Although these suppositions are plausible for NH_3BH_3 in the gas phase,[3,28,29] the orthorhombic environment does not allow a C_3 axis in the solid state, and thus it becomes relevant to scrutinize the validity of the approximations, and furthermore to determine why the predicted asymmetry (Table 1, third data column) is not observed in the ^{2}H NMR spectra.

The C_s symmetry of NH_3BH_3 in the orthorhombic crystal phase is implied by structural and EFG parameters that are nonlinear functions of atomic coordinates. We write the atomic coordinates as $\langle \mathbf{r}_N \rangle$, $\langle \mathbf{r}_B \rangle$, and so forth, in recognition of the fact that they represent ensemble averages, and we refer to results calculated from them as averaged coordinate parameters. The results presented in the ND column of Table 1 may be considered examples of averaged coordinate parameters.

Alternatively, structural and EFG parameters may be obtained by computing averages of the functions rather than the coordinates, for example, $\langle d_{NH}(\mathbf{r}_N, \mathbf{r}_H, ...) \rangle$ instead of $d_{NH}(\langle \mathbf{r}_N \rangle, \langle \mathbf{r}_H \rangle, ...)$, noting that in general $\langle f(\mathbf{x}) \rangle \neq f(\langle \mathbf{x} \rangle)$. Parameters derived from diffraction data are necessarily calculated with the averaged coordinate method, but through the use of discretized molecular dynamics simulations, structural and EFG parameters may also be determined by the second approach. Since NMR spectra are ensemble-averaged functions of EFG tensors, bond lengths, and bond angles, and not Cartesian coordinates, values calculated by this alternate method, which we call averaged function parameters, can be considered a truer representation of the experimental results than the averaged Cartesian coordinate parameters.

The results displayed in Tables 1 and 2 show that the averaged function approach predicts significantly less distortion from C_{3v} symmetry than the averaged coordinate method using ND data. More specifically, smaller differences are found by the averaged function calculations between in- and out-of-plane hydrogens in both EFG parameters and bond lengths, which is more consistent with ^{2}H NMR observations. In addition to finding

TABLE 1: Experimental and Calculated EFG Parameters and Bond Angles

	^{2}H NMR	optimized isolated molecule, 200 K	ND structure,[2] no environment,[a,b] 200 K	averaged function method,[a,b] 15 K	averaged function method,[a,b] 120 K
V_{zz} ($\times 10^{21}$ V/m^2), H−B	1.652 ± 0.082	1.902	2.597 (0.334)	1.654 (−0.098)	1.664 (−0.083)
η, H−B	0.00 ± 0.05	0.12	0.10 (−0.02)	0.02 (−0.04)	0.03 (−0.03)
∠NBH (deg)	111.2 ± 0.9	106.1	113.9 (2.4)	107.4 (−1.0)	107.4 (−1.0)
V_{zz} ($\times 10^{21}$ V/m^2), H−N	2.883 ± 0.144	3.472	2.360 (−2.850)	3.198 (0.231)	3.181 (0.216)
η, H−N	0.00 ± 0.05	0.06	0.09 (0.02)	0.02 (−0.02)	0.03 (−0.01)
∠BNH (deg)	110.3 ± 1.0	111.6	106.1 (−4.9)	112.5 (1.3)	112.6 (1.3)

[a] Parameters for mirror plane deuteron. [b] In parentheses: difference in parameters between mirror plane and out-of-plane deuterons.

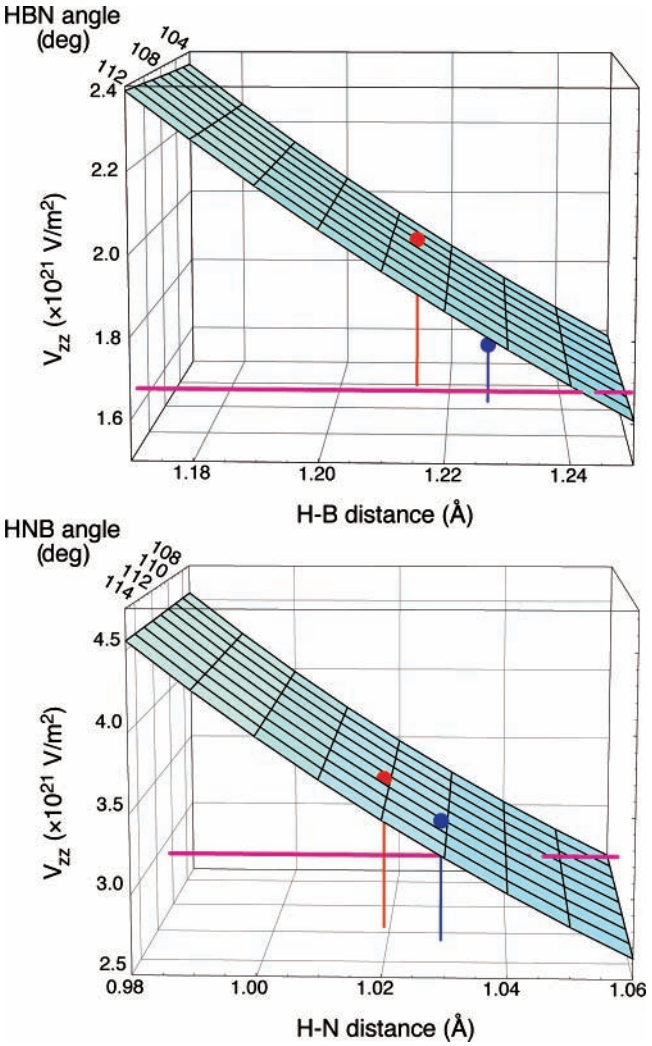

Figure 3. Dependence of the hydrogen V_{zz} on bond length and angle for an isolated molecule with C_{3v} symmetry. Top: Hypersurface for borane hydrogens. Bottom: hypersurface for amine hydrogens. Vertices on the surface mesh signify actual calculated values of V_{zz}. Also plotted are points corresponding to the optimized, symmetric, isolated molecule (red) and the averaged function calculation (blue). Deuterium NMR measurements provide values for V_{zz} and bond angles (Table 1), represented by the magenta lines.

more symmetric structures than the averaged coordinate method, the averaged function method gives results for V_{zz} and η that come closer to the values measured by NMR spectroscopy.

Environmental Effects. The evidence of C_{3v} symmetry and the weak dependence of bond lengths on temperature seen in Table 2 suggest that the geometry, and hence electronic properties, of NH_3BH_3 are largely insensitive to its environment in the orthorhombic phase. The magnitude of the influence of the environment on the EFG tensor can be assessed by the calculations summarized in Table 3. Two variants of the molecular structure determined from the ND study of Klooster et al.[2] are considered in this table: the original asymmetric structure and a symmetrized version constructed by averaging the bond lengths and angles of the original structure. The EFG tensors were calculated twice for both structures, first as an isolated molecule, and second as a molecule embedded in a cluster with eight structurally identical nearest neighbors. In the latter case, the 9 molecule cluster is contained within an orthorhombic cell with dimensions 1.4 times longer in the *a*, *b*, and *c* directions than the unit cell lengths. The B and N coordinates from the diffraction data were used to arrange both clusters.

The results presented in Table 3 reveal that the noncovalent interactions with neighboring molecules produce only small changes in the hydrogen EFG parameters. For the two structures considered, the inclusion of neighbors causes no more than a 3% change in the hydrogen V_{zz} in both the borane and the amine groups. The insensitivity of the EFG tensor to the formation of dihydrogen bonds[2] represents a notable contrast with the situation in traditional hydrogen bonds, where a strong dependence of the V_{zz} on the separation of the oxygen atoms sharing the hydrogen atom is usually observed.[30]

In view of these and the averaged parameter calculations, the NH_3BH_3 molecule appears to maintain a rigid C_{3v} symmetric structure in the orthorhombic unit cell, with minor differences in bond lengths relative to the gas phase. It can also be surmised that structural and EFG parameters will be insensitive to minor shifts in the relative positions of molecules in the unit cell, as occur when the temperature is varied. Evidence of this temperature invariance may be seen in the average parameter data in Tables 1 and 2, which show little difference in the EFG parameters and bond lengths computed for $T = 15$ and 120 K.

Dynamical ^{2}H Line Shape Analysis. Figures 2 and 4 display a series of spectra for ND_3BH_3 that extends the temperature range of the study by Penner et al.[5] down to the static limit. A similar extended range measurement was also performed for NH_3BD_3, with results that paralleled the previous findings. In the absence of spectra at the static limit, values of V_{zz} and η had previously been inferred from spectra measured in the high temperature, fast exchange limit. The direct determination of EFG parameters from the static spectra (Table 1) is found to give values for V_{zz} that differ by 8.1% for H−B and 0.7% for H−N from the results obtained by the previous analysis.

By assuming that the temperature dependence of the ^{2}H NMR lineshape is due to rotations about the B−N bond, the bond angles ∠BNH and ∠NBH can be related to the apparent V_{zz} values measured in the static and fast exchange limits. For $\eta = 0$ and B−H (and N−H) aligned with the *z* principal axis of the hydrogen EFG tensor, the ratio of the two quantities is given by the relation[15]

$$V_{zz}^{\text{fast}}/V_{zz} = \frac{1}{2}(3\cos^2\alpha - 1) \qquad (1)$$

TABLE 2: Experimental and Calculated Bond Lengths (Angstroms)

	ND structure[2], 200 K	optimized isolated molecule, 200 K	averaged function method, 15 K	averaged function method, 120 K
H−B[a,b]	1.154 (−0.027)	1.214	1.227 (−0.006)	1.228 (−0.005)
H−N[a,b]	1.074 (0.114)	1.019	1.029 (0.004)	1.030 (0.004)
B−N	1.585	1.585[c]	1.599	1.603

[a] Bond for mirror plane hydrogen. [b] In parentheses: difference in lengths between mirror plane and out-of-plane hydrogens. [c] Bond length fixed to the ND experimental value as described in Computational Methods.

TABLE 3: Effect of Environment on Calculated Hydrogen EFG Tensors

	ND structure[2]		Symmetrized structure	
	isolated molecule[a,b]	in cluster[a,b]	isolated molecule	in cluster[a,b]
V_{zz} ($\times 10^{21}$ V/m^2), H−B	2.597 (0.334)	2.562 (0.283)	2.510	2.474 (−0.043)
η, H−B	0.10 (−0.02)	0.00 (−0.05)	0.11	0.01 (−0.05)
V_{zz} ($\times 10^{21}$ V/m^2), H−N	2.360 (−2.850)	2.287 (−2.799)	3.993	3.900 (0.054)
η, H−N	0.09 (0.02)	0.03 (−0.02)	0.08	0.04 (−0.01)

[a] Parameter for mirror plane hydrogen. [b] In parentheses: difference in parameters between mirror plane and out-of-plane hydrogens.

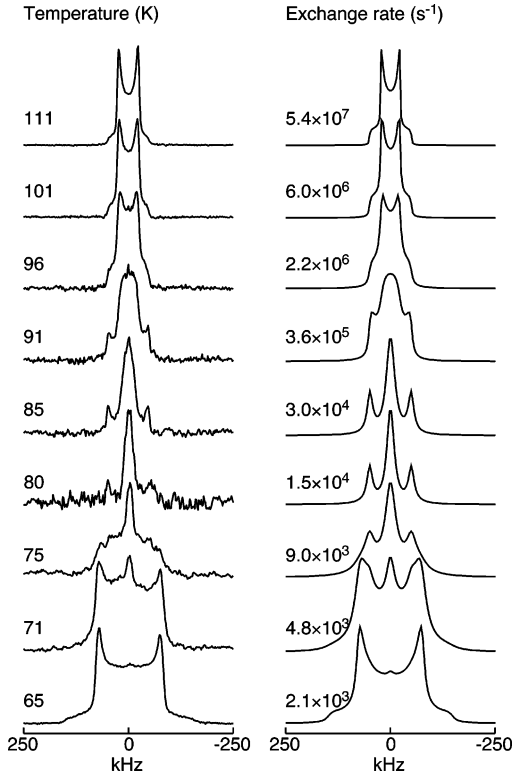

Figure 4. Experimental ^{2}H NMR quadrupolar echo spectra of ND_3BH_3 as a function of temperature (left), and best match lineshape simulations with the C_3-symmetric discrete hop model (right). The lineshape ceases to change below 60 K and above 115 K.

where α is the bond angle and V_{zz}^{fast} is the motionally averaged field gradient measured from the fast exchange spectrum. We note that the validity of eq 1 depends on V_{zz} being a constant function of temperature, which is supported by the discussion of the preceding section.

The angles ∠BNH and ∠NBH (Table 1) obtained in this way are seen to be higher than the value of 109.5° assumed by Penner et al. in their calculation of V_{zz} from V_{zz}^{fast}. By adjusting their analysis by substituting the angles in Table 1 in place of 109.5°, the V_{zz} values previously computed by Penner et al. are increased to 1.668×10^{21} V/m^2 ($eQV_{zz}/h = 115.3$ kHz) and 2.983×10^{21} V/m^2 (206.3 kHz), for B−H and N−H, respectively. The adjustment brings the previous V_{zz} result for B−H into virtual agreement with the value obtained in the present work (Table 1), while slightly widening the difference in V_{zz} values for N−H to 3.5%, which is still less than the experimental uncertainty.

As discussed in the preceding sections, ^{2}H lineshapes in NH_3BH_3 are altered by heteronuclear dipolar couplings to B and N. Insofar as the *z* principal axes of the axially symmetric dipolar and quadrupolar tensors are collinear, the magnitude of the dipolar interaction should be scaled by the same factor as the quadrupolar interaction, as given by eq 1. It is to be expected, therefore, that the resonances from the high temperature, fast exchange regime (Figure 4) should be scaled replicas of the lines in the low temperature, static limit (Figures 1 and 2). Instead, it is seen that the distortions caused by dipolar couplings are absent in the fast exchange spectra and the lineshapes converge to a classic Pake form[15] indicative of purely quadrupolar broadening. We attribute the disappearance of the dipolar interactions to the self-decoupling of ^{14}N and the B isotopes,[26] which becomes effective as the temperature increases and relaxation times of these nuclei become shorter. Quadrupolar coupling constants of 1.504 and 1.253 MHz have been reported for ^{11}B and ^{14}N, respectively, in the tetragonal phase of NH_3BH_3;[27] with values of this magnitude, it is plausible that quadrupolar mechanisms, which are proportional to $(eQV_{zz}/h)^2$, would lead to sufficiently short T_1 times to self-decouple these nuclei.

The simulated spectra in Figure 4 are from a model that assumes the C_3 molecular symmetry inferred in the previous sections and discrete hops between the three sites, for both the BH_3 and the NH_3 groups. The results of fitting the exchange rates determined with this model to an Arrhenius equation

$$k(T) = A\, e^{-E_a/k_B T} \qquad (2)$$

are shown in Figure 5 and Table 4. The data for NH_3 exhibit an apparent discontinuity between 80 and 85 K, and have been fit by separate Arrhenius functions above and below the inflection point. A fit of the NH_3 data to a sum of two exponentials leads to similar parameters ($A_1 = 1.4 \times 10^8$ s^{-1}, $E_a^{(1)} = 6.2$ kJ/mol, $A_2 = 1.6 \times 10^{17}$ s^{-1}, $E_a^{(2)} = 20.4$ kJ/mol) as the separated single exponentials regression analysis but with a slightly worse quality of fit. Results from the study of Penner et al. are also included in Table 4; of the data in this table, only the BH_3 values in the fourth and fifth columns are comparable in both experimental method and temperature range. The parameter *A* is problematic to fit numerically without points from the inaccessible high-temperature asymptote of $k(T)$, and for these data sets, we estimate the uncertainty in determining

TABLE 4: Arrhenius Parameters (cf. Eq 2) Determined by ^{2}H NMR Spectroscopy with the C_3-Symmetric Discrete Hop Model

	NH_3			BH_3		
	present work		ref 5	present work	ref 5	
	$T \leq 80$ K[a]	$T \geq 85$ K[a]	$T \geq 110$ K[b]	$T \geq 100$ K[a]	$T \geq 110$ K[a]	$T \geq 110$ K[b]
E_a (kJ/mol)	5.8 ± 0.2	22.4 ± 1.3	13.7 ± 0.9	27.2 ± 2.1	25 ± 2	26.4 ± 1.4
A (s^{-1})	8.2×10^7	2.4×10^{18}	5.8×10^{13}	3.6×10^{16}	7.0×10^{17}	2.8×10^{16}

[a] From analysis of lineshape temperature dependence. [b] From analysis of spin−lattice relaxation time temperature dependence.

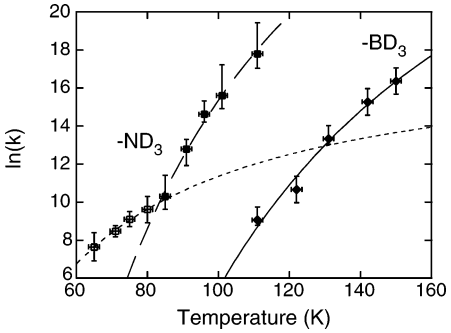

Figure 5. Temperature dependence of the exchange rates determined with the C_3-symmetric discrete hop model and nonlinear least-squares fits of the data to an Arrhenius function. Open squares and dotted curve: data and fit for ND_3BH_3, $T \leq 80$ K. Solid squares and dashed curve: data and fit for ND_3BH_3, $T \geq 85$ K. Solid diamonds and solid curve: data and fit for NH_3BD_3.

A to span a two decade range. Therefore, we focus on comparing activation energies, which can be more accurately evaluated with the limited range of points available. For the BH_3 studies, we find good agreement among E_a measurements. Recent DFT calculations[31] have shown that the differences in activation energies between BH_3 and NH_3 can be attributed in part to the stronger interactions of BH_3 with the environment through intermolecular dihydrogen bonding.

Deuterium spin−lattice relaxation times may be used to determine correlation times of hydrogen motion, and thus variable-temperature T_1 measurements provide an alternative way for extracting the Arrhenius parameters A and E_a. Such an approach has been tried in the case of NH_3BH_3 rotation (ref 5 and Table 4). Theoretical complications with this method arise when the motion of the hydrogen is anisotropic and characterized by jumps between discrete sites, which lead to relaxation times that are highly orientation dependent.[32] Interpretation of the temperature dependence of the ^{2}H T_1 in the solid state is further complicated by the necessity of using spin-echoes to detect the magnetization in inversion recovery experiments. Because signal dephasing caused by stochastic motion cannot be refocused in an echo experiment, a non-representative fraction of the ^{2}H nuclei in a polycrystalline sample is detected by this technique, depending on the hop rates, trajectory of the motion, and refocusing time of the echo sequence.[16] We have observed reductions in signal intensity of greater than a factor of 10^2 in measurements on NH_3BH_3 at temperatures where the correlation time of the motion becomes approximately equal to the refocusing time. These factors suggest that Arrhenius parameters obtained by the relaxation time method and the dynamical lineshape analysis may not be directly comparable, and offer a possible explanation for the variation in NH_3 results.[4−6]

We have repeated the variable temperature T_1 measurements of Penner et al.[5] and extended the lower limit of the range from 115 to 10 K (see Supporting Information). Good agreement was found at the overlapped temperatures. Correlation times extracted by the simplified quadrupolar relaxation model of Bloembergen, Purcell, and Pound (BPP)[15,32,33] are found to exhibit significant and systematic departures from an Arrhenius temperature dependence for both the amine and the borane deuterons. We ascribe the anomalous behavior to the factors listed above, and note additionally that the classical BPP expressions assume random isotropic reorientation of the quadrupolar moment, in contrast to the discrete rotations of deuterons in solid NH_3BH_3.

5. Conclusion

Proper treatment of the effects of statistical averaging is shown to be crucial in the interpretation of ^{2}H NMR results and the elucidation of molecular structure and dynamics in the low-temperature phase of NH_3BH_3. Straightforward use of atomic Cartesian coordinates to compute EFG tensors, bond lengths, and bond angles leads to inconsistencies with NMR observations that can be attributed to the inappropriateness of using averaged variables to derive an average of a nonlinear function of the variables.

In the case of the orthorhombic phase of NH_3BH_3, the averaged coordinates from diffraction experiments imply an asymmetric structure that is at variance with the C_3 symmetry indicated by the ^{2}H NMR spectra. Statistical calculations show that the discrepancy is resolved when EFG and structural parameters are computed as ensemble averages, rather than as functions of a single set of averaged Cartesian coordinates. The averaging process results in EFG parameters that are also in better agreement with experimental measurements.

The structure of the NH_3BH_3 molecule that emerges from this viewpoint is much closer to C_{3v} symmetry than the structure derived from diffraction-based coordinates, which suggests that the molecule largely retains its symmetric gas-phase structure in the orthorhombic unit cell.

Acknowledgment. Benjamin Schmid assisted in preliminary NMR measurements. This work was supported by the U.S. Department of Energy, Office of Science, Basic Energy Sciences, Chemical Sciences Division. The Pacific Northwest National Laboratory is operated for the U.S. Department of Energy by the Battelle Memorial Institute under Contract No. DE-AC05-76RL01830.

Supporting Information Available: Author list for ref 17; variable-temperature ^{2}H spin−lattice relaxation (T_1) data. This material is available free of charge via the Internet at http://pubs.acs.org.

References and Notes

(1) (a) Wolf, G.; Baumann, J.; Baitalow, F.; Hoffmann, F. P. *Thermochim. Acta* **2000**, *343*, 19−25. (b) Gutowska, A.; Li, L.; Shin, Y.; Wang, C. M.; Li, X. S.; Linehan, J. C.; Smith, R. S.; Kay, B. D.; Schmid, B.; Shaw, W.; Gutowski, M.; Autrey, T. *Angew. Chem., Int. Ed.* **2005**, *44*, 3578−3582. (c) Stowe, A. C.; Shaw, W. J.; Linehan, J. C.; Schmid, B.; Autrey, T. *Phys. Chem. Chem. Phys.* **2007**, *9*, 1831−1836 (d) Bluhm, M. E.; Bradley, M. G.; Butterick, R.; Kusari, U.; Sneddon, L. G. *J. Am. Chem. Soc.* **2006**, *128*, 7748−7749. (e) Stephens, F. H.; Pons, V.; Baker, R. T. *Dalton Trans.* **2007**, 2613−2626. (f) Marder, T. B. *Angew. Chem., Int. Ed.* **2007**, *46*, 8116−8118.

(2) (a) Klooster, W. T.; Koetzle, T. F.; Siegbahn, P. E. M.; Richardson, T. B.; Crabtree, R. H. *J. Am. Chem. Soc.* **1999**, *121*, 6337−6343. (b) Allis, D.; Kosmowski, M. E.; Hudson, B. S. *J. Am. Chem. Soc.* **2004**, *126*, 7756−7757.

(3) Thorne, L. R.; Suenram, R. D.; Lovas, F. J. *J. Chem. Phys.* **1983**, *78*, 167−171.

(4) Reynhardt, E. C.; Hoon, C. F. *J. Phys. C* **1983**, *16*, 6137−6152.

(5) Penner, G. H.; Chang, Y. C. P.; Hutzal, J. *Inorg. Chem.* **1999**, *38*, 2868−2873.

(6) Gunaydin-Sen, O.; Achey, R.; Dalal, N. S.; Stowe, A.; Autrey, T. *J. Phys. Chem. B* **2007**, *111*, 677−681.

(7) Lipton, A. S.; Heck, R. W.; Sears, J. A.; Ellis, P. D. *J. Magn. Reson. A* **2004**, *168*, 66−74.

(8) Slichter, C. P. *Principles of Magnetic Resonance*, 3rd Ed.; Springer-Verlag: New York, 1990.

(9) Samoson, A.; Kundla, E.; Lippmaa, E. *J. Magn. Reson.* **1982**, *49*, 350−357.

(10) Mehring, M. *Principles of High Resolution NMR in Solids*, 2nd Ed.; Springer-Verlag, Berlin, 1983.

(11) Mombourquette, M. J.; Weil, J. A. *J. Magn. Reson.* **1992**, *99*, 37−44.

(12) Raghavan, P. *Atom. Data Nucl. Data Tables* **1989**, *42*, 189−291.

(13) Smith, S.; Levante, T.; Meier, B. H.; Ernst, R. R. *J. Magn. Reson. A* **1994**, *106*, 75−105.

(14) Anderson, P. W. *J. Phys. Soc. Jpn.* **1954**, *9*, 316−339.

(15) Abragam, A. *Principles of Nuclear Magnetism*; Clarendon: Oxford, 1961.

(16) (a) Greenfield, M. S.; Ronemus, A. D.; Vold, R. L.; Vold, R. R.; Ellis, P. D.; Raidy, T. E. *J. Magn. Reson.* **1987**, *72*, 89−107. (b) Schmidt-Rohr, K.; Spiess, H. W. *Multidimensional Solid-State NMR and Polymers*; Academic Press: San Diego, 1994.

(17) Gaussian 98, Revision A.7; Frisch, M. J. et al. Gaussian, Inc.; Pittsburgh, PA, 1998.

(18) Becke, A. D. *J. Chem. Phys.* **1993**, *98*, 5648−5652.

(19) (a) Hehre, W. J.; Ditchfield, R.; Pople, J. A. *J. Chem. Phys.* **1972**, *56*, 2257−2261. (b) Dill, J. D.; Pople, J. A. *J. Chem. Phys.* **1975**, *62*, 2921−2923. (c) Francl, M. M.; Pietro, W. J.; Hehre, W. J.; Binkley, J. S.; Gordon, M. S.; DeFrees, D. J.; Pople, J. A. *J. Chem. Phys.* **1982**, *77*, 3654−3665.

(20) Lippert, G.; Hutter, J.; Parrinello, M. *Mol. Phys.* **1997**, *92*, 477−487.

(21) Vande Vondele, J.; Krack, M.; Mohamed, F.; Parrinello, M.; Chassaing, T.; Hutter, J. *Comput. Phys. Commun.* **2005**, *167*, 103−128.

(22) Perdew, J. P.; Burke, K.; Ernzerhof, M. *Phys. Rev. Lett.* **1996**, *77*, 3865−3868.

(23) Goedecker, S.; Teter, M.; Hutter, J. *Phys. Rev. B* **1996**, *54*, 1703−1710.

(24) Hartwigsen, C.; Goedecker, S.; Hutter, J. *Phys. Rev. B* **1998**, *58*, 3641−3662.

(25) Hess, N. J.; Schenter, G. K.; Stowe, A. C.; Daemen, L. L.; Proffen, T.; Autrey, S. T., manuscript in preparation.

(26) Spiess, H. W.; Haeberlen, U.; Zimmermann, H. *J. Magn. Reson.* **1977**, *25*, 55−66.

(27) Lötz, A.; Voitländer, J. *J. Magn. Reson.* **1982**, *48*, 1−8.

(28) Binkley, J. S.; Thorne, L. R. *J. Chem. Phys.* **1983**, *79*, 2932−2940.

(29) Dixon, D. A.; Gutowski, M. *J. Am. Chem. Soc.* **2005**, *109*, 5129−5135.

(30) Berglund, B.; Vaughan, R. W. *J. Chem. Phys.* **1980**, *73*, 2037−2043.

(31) Parvanov, V. M.; Schenter, G. K.; Hess, N. J.; Daemen, L. L.; Hartl, M.; Stowe, A. C.; Camaioni, D. M.; Autrey, T. *Dalton Trans.*, in press.

(32) Torchia, D. A.; Szabo, A. *J. Magn. Reson.* **1982**, *49*, 107−121.

(33) Bloembergen, N.; Purcell, E. M.; Pound, R. V. *Phys. Rev.* **1948**, *73*, 679−712.